ELSEVIER

Chemical Engineering Journal 137 (2008) 62–71

Chemical Engineering Journal

www.elsevier.com/locate/cej

Hydroxyapatite/β-tricalcium phosphate/agarose macroporous scaffolds for bone tissue engineering

S. Sánchez-Salcedo, A. Nieto, M. Vallet-Regí*

Departamento de Química Inorgánica y Bioinorgánica, Facultad de Farmacia, Universidad Complutense de Madrid, 28040 Madrid, Spain

Received 28 May 2007; received in revised form 5 September 2007; accepted 6 September 2007

Abstract

Designed porous architecture scaffolds have been prepared with an innovative combination of techniques, avoiding the sintering stage for tissue engineering application. Firstly, hydroxyapatite/β-tricalcium phosphate HA/β-TCP/agarose porous scaffolds have been manufactured using a homogeneous ceramic/agarose suspension at low temperature, leading to non designed architecture scaffolds. In order to achieve scaffolds for bone tissue engineering applications a polymeric negative, obtained by stereolithography technique, is filled with this suspension. Afterwards, the polymeric negative is eliminated by alkaline dissolution at room temperature in order to obtain the designed architecture scaffolds. Secondly, room temperature and freeze-drying techniques have been applied in scaffolds drying stage. In this way, strong dried scaffolds, fully interconnected with high porosity, thoroughly open pores and tailored pore size have been obtained. Besides, depending on the drying technique employed, different porosity (59–80%), distribution of pores size (∼0.2 and 70 μm) and interconnected three-dimensional ellipsoidal channels between 300 μm × 380 μm and 340 μm × 460 μm can be achieved. In contact with body fluids, these scaffolds show flexibility and capacity to exert pressure into the bone defect of the patient and be easily handled by the surgeon.

Keywords: Low temperature method; Stereolithography; Designed architecture; Porous scaffold; Biodegradable

1. Introduction

Tissue engineering offers a promising new approach to regenerate diseased or injured tissues such as bone [1]. For that issue, three dimensional biocompatible porous scaffolds with a highly interconnected porosity are designed in order to allow cell migration, vascularization and diffusion of nutrients [2,3]. From a macroscopic point of view, bone tissue is non-homogeneous, porous and anisotropic. Two types of bone tissue can be distinguished: *trabecular or cancellous* and *cortical or compact*. It is feasible to design the porosity of the materials to be similar to that of trabecular bone which has a 50–95% of porosity and a network of interconnected pores [3]. In this sense, it is of great interest to obtain pore diameters of a hundred microns [4–6] and a number of designed pore interconnections to verify in the shortest possible time a bioresorption of the scaffold and the subsequent new bone formation. For this purpose, it is necessary to design highly porous scaffolds, which must include the necessary macroporosity to ensure bone oxygenation and angiogenesis [7]. Therefore, designed porous scaffolds should have a network of interconnected pores where more than 60% of pores should have a size ranging from 150 to 400 μm and, at least 20% should be smaller than 20 μm. Pores with sizes of less than 1 μm are appropriate to interact with proteins and are the main responsibles for bioactivity. On the other hand, pores with sizes between 1 and 20 μm are important in cellular development, type of cells attracted and orientation and directionality of cellular ingrowth. Moreover, pores of sizes between 100 and 1000 μm play an important role in cellular and bone ingrowth, being necessary for blood flow distribution and having a predominant function in the mechanical strength of the substrate. Finally, the presence of pores of sizes greater than 1000 μm will have an important role in the implant functionality and in its shape and esthetics. Consequently, porosity of three-dimensional scaffolds is a very important matter due to its great influence on the implant final behaviour.

Existing methods for manufacturing reliable interconnected porous scaffolds are mainly based on the incorporation of poro-

* Corresponding author. Tel.: +34 91 394 1861; fax: +34 91 394 1786.
E-mail address: vallet@farm.ucm.es (M. Vallet-Regí).

1385-8947/$ – see front matter © 2007 Elsevier B.V. All rights reserved.
doi:10.1016/j.cej.2007.09.011

Nomenclature

V_d	volume of dried scaffolds
V_o	volume of just prepared scaffolds
V_t	volume of rehydrated scaffolds at time t
W_d	weight of dried scaffolds
W_o	weight of just prepared scaffolds
W_t	weight of rehydrated scaffolds at time t

gen particles [8–10], the use of polymer sponge methods [11,12], gel-casting of foams [13] and cold isostatic pressing [14]. Such methods require two steps, firstly, the pirolyzation of the organic phases such as porogens, binders, dispersing agents, etc. and secondly, a sintering treatment of scaffolds in order to generate a macroporous system. Moreover, these processes entail a difficult control of pores interconnection and the uniformity of pore size.

However, from the point of view of biomaterials field, it is interesting to manufacture macroporous scaffolds with controlled and designed pore architecture [15] and without a thermal treatment step required. Traditional procedures for the manufacturing of ceramic pieces imply thermal treatment steps. However, in this case a thermal step is not advisable because it would exponentially increase the particle size and the crystallinity of the ceramic matrix [16]. This creates scaffolds with enough consistency to be implanted by the surgeon.

A good approach could be based on the combination of the solid free form (SFF) fabrication method, that leads to a negative epoxy resin mould of the scaffold generated by stereolithography [17], with a low temperature shaping method. In order to produce macroporosity, the epoxy resin should be eliminated with solvents. Besides, the final scaffold must be biocompatible and not cytotoxic.

Biphasic calcium phosphate (BCP), consisting of HA and β-TCP, represent two of the main types of calcium phosphates used in orthopaedic repair and maxillofacial applications [7,16,18]. They show excellent biocompatibility and bioactivity and have the ability to promote osteoconduction [19–21]. Therefore, this BCP bioceramic has been selected as ceramic matrix.

Agarose, a biodegradable polymer, has been selected as organic matrix because it is a biocompatible hydrogel which acts as gelling agent leading to strong gels and fast room temperature polymerization. It exhibits macromolecular properties similar to the extracellular matrix, and allows enough diffusion and transport of oxygen, essential nutrients and secretary products across its network [22,23].

Therefore, the development of scaffolds based on organic–inorganic matrices combines the properties of both types of materials.

The purpose of the current work was to manufacture porous scaffolds using HA/β-TCP as ceramic matrix and agarose as a binder, combined with the stereolithography technique employing room temperature and freeze-drying techniques in the drying step in order to obtain designed architecture porous scaffolds.

2. Materials and methods

2.1. Starting materials

2.1.1. Ceramic component

The ceramic component is a BCP that consist of a mixture of HA and β-TCP. The bioreactivity of this BCP can be increased by increasing the β-TCP/HA ratio. Therefore, the solubility of the scaffold can be controlled through the phase composition. BCP bioceramics are recommended for use as an alternative or additive to autogenous bone for orthopaedic and dental applications due to their bioactive behaviour and excellent biocompatibility. However, the limiting factor in the use of BCP bioceramics is their inherent brittleness, making them unsuitable for load-bearing applications.

In the present work, calcium phosphate deficient apatite powder, which can be formulated as: $Ca_{9.27}(HPO_4)_{0.73}(PO_4)_{5.27}(OH)_{1.27}$, was prepared by aqueous precipitation reaction as described previously [24,25]. Briefly, $Ca(NO_3)_2{\cdot}4H_2O$ (0.92 M) and $(NH_4)_2HPO_4$ (0.60 M) (Aldrich, Steinheim, Germany) were dropped simultaneously at 50 °C and pH 7.1. Then, the obtained powder was thermally treated at 900 °C for 1 h, giving rise to a biphasic calcium phosphate that consists of 26.9% HA and 73.1% β-TCP. The particle size distribution was $d_{0.1} = 1.0$ μm, $d_{0.5} = 3.9$ μm and $d_{0.9} = 21.2$ μm and the specific surface area 8.0 m^2/g.

2.1.2. Organic component

Agarose (for routine use, Sigma–Aldrich) is a biocompatible and biodegradable natural polymer, which acts as gelling agent leading to strong gels and allowing fast room temperature polymerization.

2.2. Combination of ceramic component (HA/β-TCP) with the organic component (agarose)

The mixture of HA/β-TCP and agarose allows the combination of the properties of biocompatibility and bioactivity of the ceramic matrix with the flexibility, wettability and biodegradability of agarose hydrogel.

In order to prepare a mixture of both components, agarose was dissolved in distilled water to get a solution of 5% (w/v) at 85–90 °C. Concentrations of 8, 20, 24 and 28% (w/v) of HA/β-TCP powder were then added to the agarose solution and the mixture stirred at 60 °C.

The viscosity of the slurries was measured in a Haake ReoStress RS75 rheometer with a cone–plate system, in the shear rate range of 1–700 s^{-1} at 60 °C. In order to analyse the effect of temperature on the viscosity of the suspensions, measurements were performed at a shear rate of 300 s^{-1} on cooling from 70 to 30 °C.

Once selected the appropriate composition of HA/β-TCP/agarose suspension, the manufacturing of pieces was carried out following a low temperature shaping method. This method consists in pouring the HA/β-TCP/agarose suspension into cylindrical-shaped moulds. The suspension is allowed to polymerize at room temperature for about 10 min. After that,

the samples are removed from the moulds. Then the obtained pieces are dried at room temperature (RT) leading to pieces named as (HA/β-TCP)/Aga-RT (Fig. 1). Nevertheless, these systems only represent a preliminary step in the design of scaffolds with applications in bone tissue engineering. For this purpose, a designed and controlled interconnected macroporosity is necessary.

2.3. Alternative to obtain HA/β-TCP/agarose designed porous architecture scaffolds

In order to obtain designed porous architecture scaffolds for its application in bone regeneration, the innovative combination of the low temperature method for shaping HA/β-TCP/agarose mixtures with the stereolitography technique is an excellent choice.

The stereolithography technique has been previously described [26]. Briefly, it is a computer-controlled fabrication technique for generating three-dimensional objects by forming successive cross-sectional laminae, one on top of another. A programmed movable spot beam of UV light shining on a layer of a photocurable polymer is used to form a solid cross-section of the object. The object is then moved, in a programmed manner, away from the liquid surface by the thickness of one layer, and the next cross-section is then formed and adhered to the immediately preceding layer defining the epoxy resin negative, till the whole object is shaped.

For the preparation of designed porous architecture scaffolds a HA/β-TCP/agarose mixture was poured into cylindrical-shaped moulds. In order to obtain pieces of HA/β-TCP/agarose with a designed architecture (DA), the moulds were filled with an epoxy resin negative (Accura^{TM} SI10 System, Germany) previously designed by stereolithography (Fig. 1). The just prepared scaffolds with epoxy resin negatives were immersed in a 2 M NaOH solution during 22 h in order to eliminate the polymer. Once the polymer was completely removed, scaffolds were washed with distilled water until neutral pH leading to DA-(HA/β-TCP)/Aga samples. Finally, the DA scaffolds were dried in two ways: at room temperature and by freeze-drying (FD) for 24 h giving rise to scaffolds named as DA-(HA/β-TCP)/Aga-RT and DA-(HA/β-TCP)/Aga-FD, respectively.

2.4. Characterization of HA/β-TCP/agarose scaffolds

Powder X-ray diffraction (XRD) was carried out with a Philips X'Pert diffractometer by using Cu Kα radiation, in order to determine the quantitative phase composition of ceramic matrix of scaffolds. The XRD patterns were refined by the Rietveld method using FullProf software [27]. Previously reported structural data for HA [28] and β-TCP [29] were used as initial model for Rietveld refinements.

Thermogravimetric (TG) analyses were carried out with a Perkin-Elmer Pyris Diamond TG/DTA instrument, between 30 and 600 °C in air at a flow rate of 100 ml/min and a heating rate of 10 °C/min.

Scanning electron microscopy and energy dispersive X-ray spectroscopy (SEM–EDS) were performed in a JEOL 6400 Microscope-Oxford Pentafet super ATW system.

The Hg porosimetry study was carried out by using a Micromeritics AutoPore III 9410 porosimeter.

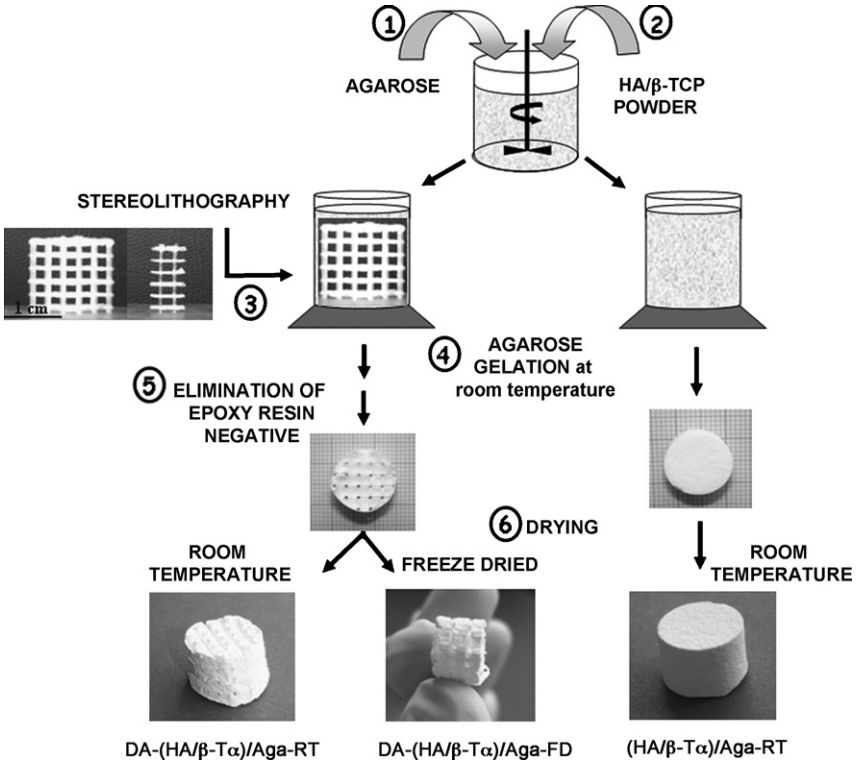

Fig. 1. Shaping method to conform the designed and non designed architecture scaffolds.

Table 1
Components, functions and content of suspensions for viscosity measurements

Component	Function	C_0 (%w/v)	C_1 (%w/v)	C_2 (%w/v)	C_3 (%w/v)	C_4 (%w/v)
HA/β-TCP	Ceramic matrix	–	8	20	24	28
Agarose	Binder	5	5	5	5	5
Water	Solvent	95	87	75	71	67

2.5. Drying and rehydration assays

The shrinkage of the (HA/β-TCP)/Aga-RT, DA-(HA/β-TCP)/Aga-RT and (DA-(HA/β-TCP)/Aga-FD samples after the drying step was calculated as:

$$\%W_{\mathrm{SHRINKAGE}} = 100 \times \frac{W_{\mathrm{o}} - W_{\mathrm{d}}}{W_{\mathrm{o}}} \quad (1)$$

$$\%V_{\mathrm{SHRINKAGE}} = 100 \times \frac{V_{\mathrm{o}} - V_{\mathrm{d}}}{V_{\mathrm{o}}} \quad (2)$$

The swelling behaviour of the HA/β-TCP/agarose samples was determined by gravimetric ($\%W$) and volumetric ($\%V$) analyses as:

$$\%W_{\mathrm{REHYDRATION}} = 100 \times \frac{W_t - W_{\mathrm{d}}}{W_{\mathrm{d}}} \quad (3)$$

$$\%V_{\mathrm{REHYDRATION}} = 100 \times \frac{V_t - V_{\mathrm{d}}}{V_{\mathrm{d}}} \quad (4)$$

The samples were placed in distilled water at 37 °C. The weight and volume of the hydrated samples were measured along time until the scaffolds reached the swelling ratio equilibrium.

3. Results and discussion

3.1. Selection of the HA/β-TCP/agarose suspension for the manufacturing of porous scaffolds

Table 1 illustrates the components, their function and the content of suspensions for viscosity measurements.

The evolution of viscosity on cooling has been tested in the range of temperatures from 70 to 30 °C (Fig. 2). In general, HA/β-TCP/agarose suspensions show a viscosity increase on cooling. Reaching the gelling temperature ($T_g \sim 36$ °C) a significant increase in viscosity occurs. It is observed that there is no change in T_g when increasing ceramic content, though viscosity increases sharply when higher HA/β-TCP powder content is added. In order to achieve the lower viscosity with the highest ceramic concentration possible and minimal water evaporation, the chosen temperature was 60 °C.

Fig. 2 shows the viscosity versus shear rate for different HA/β-TCP loadings in aqueous 5% (w/v) agarose solutions. The shape of the curves indicates a nearly Newtonian behaviour until 8% (w/v). However, for higher concentrations of HA/β-TCP, viscosity decreases with increasing shear rate. This is mainly caused by the shear-thinning behaviour of these suspensions. As can be seen, slurries with 24% (w/v) of HA/β-TCP powder follow this behaviour exhibiting a slight thixotropy, which increases when larger amounts of HA/β-TCP are added. This phenomenon occurs as a delay of structural reorganization when the solid content of suspensions is very high. Homogeneous slurries with high solid content are essential for obtaining dense and defect-free pieces. Moreover, this avoids an excessive shrinkage due to bending or cracking in the drying stage. Therefore, suspension with 24% (w/v) of ceramic powder was selected. This suspension was used to manufacture pieces following the low temperature shaping method. It is worth remarking that these systems give rise to biocompatible and biodegradable pieces with non designed porosity which present traditional biomedical applications such as bone filling and replacement. Besides, this shaping method allows to prepare scaffolds easy to manipulate with good workability for shaping complex forms and flexibility when in contact with water. These features make them appropriate to be handled in clinical practice (Fig. 3). For this purpose, *non* designed porous architecture scaffolds have been manufac-

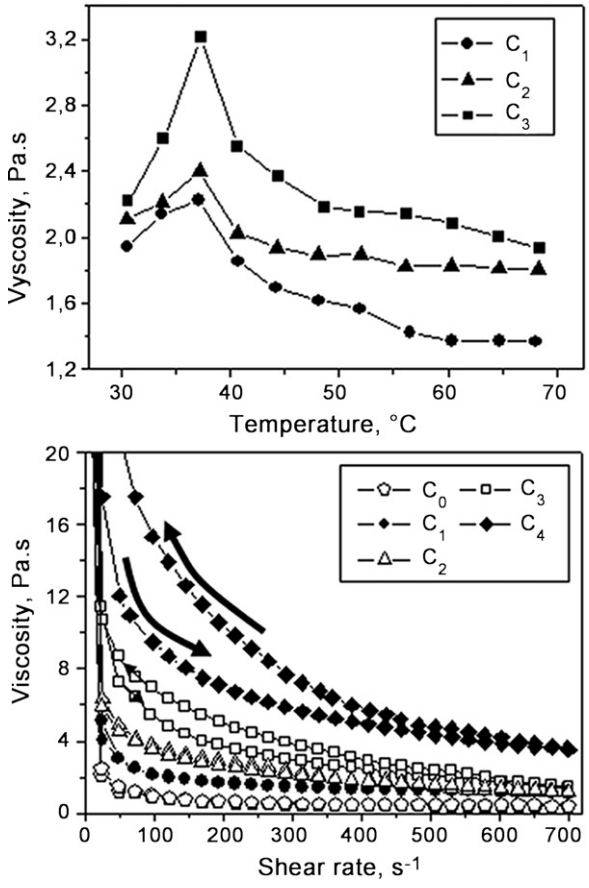

Fig. 2. Dependence of viscosity with temperature in the 70–30 °C range, for several concentrations of HA/β-TCP in 5% (w/v) of agarose solution at 300 s^{-1} (up) and shear rate (down) by ascending (→) and descending (←) shear rate ramps for different HA/β-TCP contents in agarose solution at 60 °C.

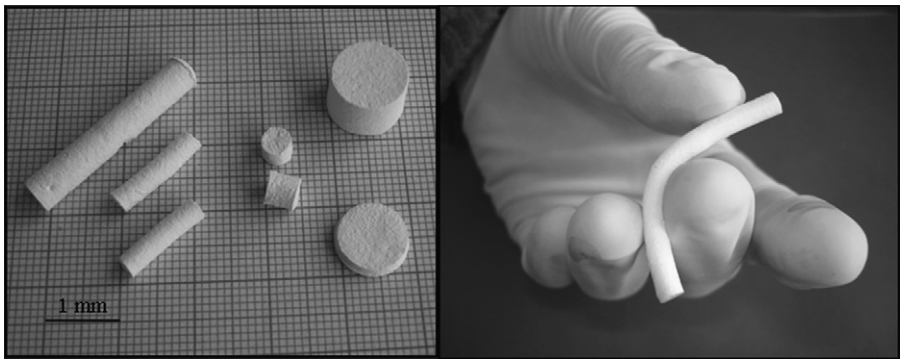

Fig. 3. Non designed architecture scaffolds: (HA/β-TCP)/Aga-RT dried at room temperature with different dimensions.

tured using a low temperature shaping method. However, to use these systems as scaffolds for bone tissue engineering, it is necessary the combination with the stereolithography technique in order to get *designed porous architecture* scaffolds, as previously explained.

3.2. Characterization of porous scaffolds

The XRD pattern of HA/β-TCP powder from DA-(HA/β-TCP)/Aga-RT after NaOH treatment and agarose elimination by calcination at 600 °C, was refined by the Rietveld method using FullProf software and compared with raw HA/β-TCP powder (Fig. 4). The refinement determines that there are neither new phases nor changes in the HA/β-TCP phase composition. This corroborates the chemical stability of the ceramic matrix along the overall process [30,31]. The XRD patterns of agarose after NaOH treatment shows the presence of Na_2CO_3 due to the reactivity of the polymer during the alkali treatment.

TG analyses allow the determination of the composition of scaffolds by calculating the total weight loss at 600 °C corresponding to the nominal organic fraction contained into the sample. Non designed and designed architecture scaffolds show 17 wt.% agarose and 83 wt.% HA/β-TCP and 15 wt.% agarose and 85 wt.% HA/β-TCP, respectively. The slight difference between them may correspond to partial degradation of agarose in the elimination step of epoxy resin.

Fig. 5 shows the surface micrographs of (HA/β-TCP)/Aga-RT and DA-(HA/β-TCP)/Aga-RT as well as the distribution of elements determined by EDS. The homogeneous distribution of C, Ca and P in both scaffolds evidences that the HA/β-

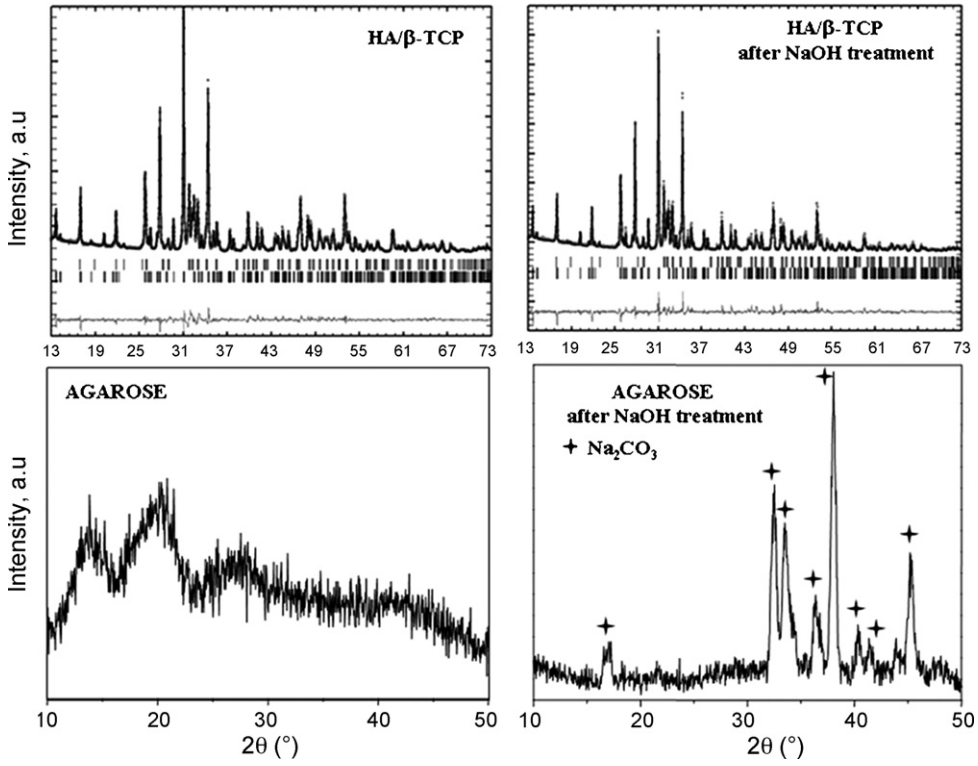

Fig. 4. Experimental (symbol) and calculated (solid line) powder X-ray diffraction patterns for: HA/β-TCP powder and HA/β-TCP powder after NaOH treatment. The vertical lines correspond to the position of HA and β-TCP phases. The lower line is the difference between experimental and calculated pattern. DRX diffraction patterns of agarose and agarose after NaOH treatment.

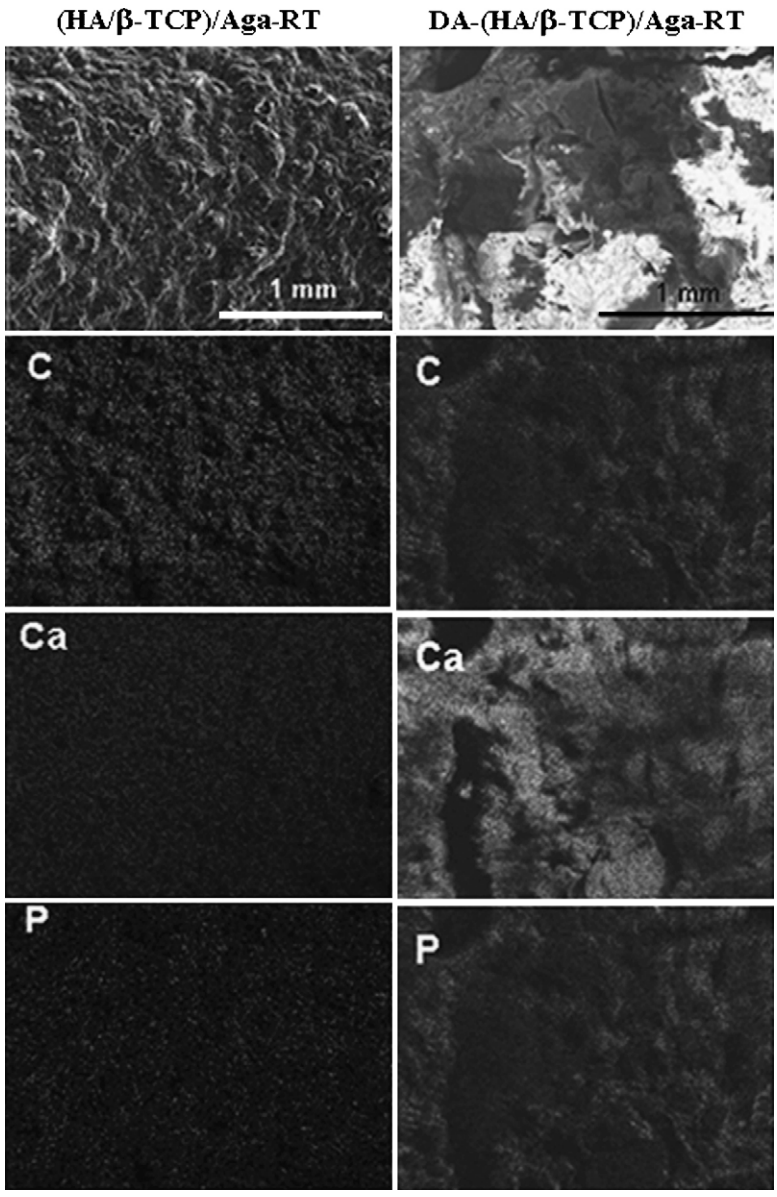

Fig. 5. SEM micrographs and C, Ca and P elements distribution of (HA/β-TCP)/Aga-RT and DA-(HA/β-TCP)/Aga-RT scaffolds.

TCP/agarose suspension selected was homogeneous enough in order to avoid agglomerates that could lead to disintegration of scaffolds.

Fig. 6a and b illustrates surface and fracture micrographs of (HA/β-TCP)/Aga-RT. A homogenous distribution of HA/β-TCP particles in the agarose hydrogel is observed. Fig. 6c and f corresponds to the surface and fracture micrographs of scaffolds with designed architecture showing the interconnected macropores left by the epoxy resin negative. On the one hand, DA-(HA/β-TCP)/Aga-RT shows ellipsoidal pores with average dimensions of 300 μm × 380 μm and an average distance between passages of 0.8 mm (Fig. 6c, d–g, h). On the other hand, DA-(HA/β-TCP)/Aga-FD micrographs show bigger ellipsoidal pores of 340 μm × 460 μm and an average distance between passages of 1.1 mm (Fig. 6e, f–i, j). This range of macroporosity is suitable for rapid vascularization and osteoconduction essential for bone remodelling [11,32,33].

As can be seen in Fig. 6k–p, a sponge-like structure formed by agarose hydrogel covers and surrounds HA/β-TCP particles. At the same time, highly porous and open pore structures without evidences of a non-porous skin layer at the outside of scaffolds are shown.

There are no significant differences between fracture micrographs of non designed architecture and designed architecture scaffolds. Nevertheless, it is worth remarking that the designed architecture scaffolds show a less rough surface without a significant degradation of agarose polymer due to NaOH treatment.

Fig. 7a exhibits the pore size distribution obtained after mercury intrusion porosimetry. The three samples show sharp maxima centred at around 0.2 μm. However, the pore size distribution of DA-(HA/β-TCP)/Aga-FD is displaced towards higher pore interconnection sizes. It is interesting to note that no pore interconnections with a diameter larger than 1 μm are present in (HA/β-TCP)/Aga-RT sample. However, DA-(HA/β-

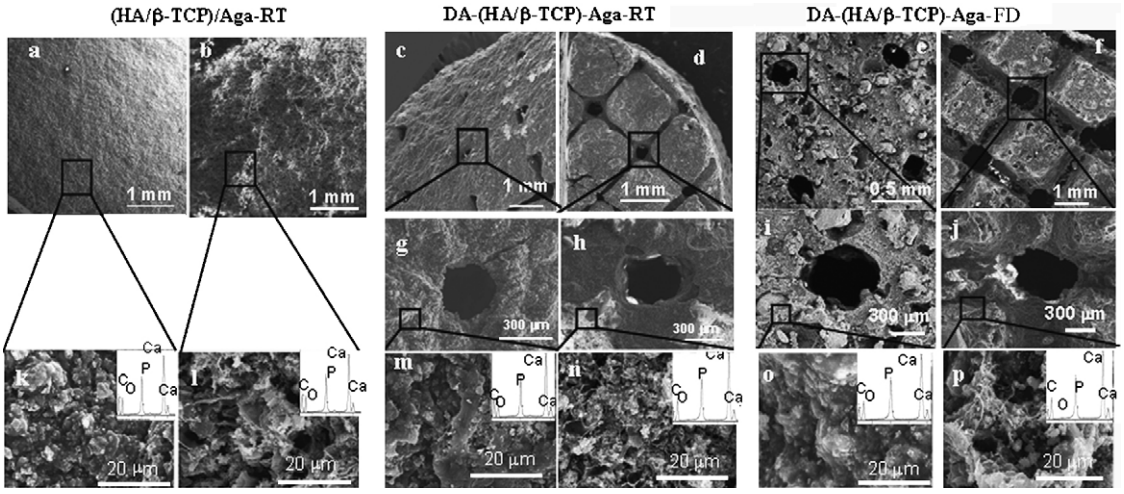

Fig. 6. SEM micrographs and EDS spectra of (a, b, h, l) (HA/β-TCP)/Aga-RT; (c, d, g, h, m, n) DA-(HA/β-TCP)/Aga-RT and (e, f, i, j, o, p) DA-(HA/β-TCP)/Aga-FD scaffolds.

TCP)/Aga-RT and DA-(HA/β-TCP)/Aga-FD samples exhibit maxima centred at 200 and 70 μm, respectively. In the case of DA-(HA/β-TCP)/Aga-RT, this maximum corresponds to the macroporosity performed by the epoxy resin negative as shown in Fig. 6. The disagreement of this data (200 μm) with the measured dimensions obtained from SEM micrographs is mainly due to the detection limit of the Hg porosimetry technique being close to that value. In the case of DA-(HA/β-TCP)/Aga-FD the maximum centred at 70 μm is attributed to the macroporosity generated by the freeze-drying technique. As can be seen in (Fig. 7b), this enables the formation of a network of open pores [34].

The total porosity of (HA/β-TCP)/Aga-RT, DA-(HA/β-TCP)/Aga-RT and DA-(HA/β-TCP)/Aga-FD samples is 59, 63 and 80%, respectively. It is interesting to note that the contribution to the 1–300 μm pore size interval is of 31% for DA-(HA/β-TCP)/Aga-FD whereas DA-(HA/β-TCP)/Aga-RT contributes with 16% and (HA/β-TCP)/Aga-RT has no contribution.

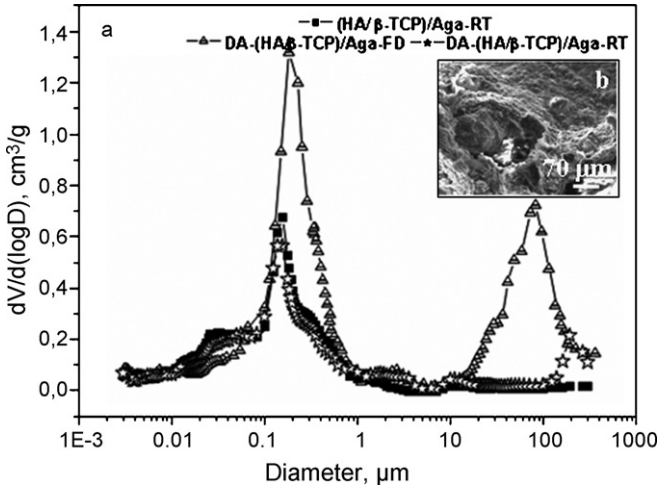

Fig. 7. (a) Pore size distribution of (HA/β-TCP)/Aga-RT, DA-(HA/β-TCP)/Aga-RT and DA-(HA/β-TCP)/Aga-FD scaffolds and (b) SEM micrograph of DA-(HA/β-TCP)/Aga-FD.

Fig. 8 illustrates DA-(HA/β-TCP)/Aga-RT and DA-(HA/β-TCP)/Aga-FD porous scaffolds of different dimensions, after epoxy resin elimination and drying by the two techniques described above.

3.3. Effect of shrinkage and rehydration of the porous scaffolds

Agarose is a polysaccharide with polar groups which make it a hydrophilic and absorbent polymer [35,36]. In order to simulate (HA/β-TCP)/Aga-RT, DA-(HA/β-TCP)/Aga-RT and DA-(HA/β-TCP)/Aga-FD behaviour in body fluid, rehydration assays have been carried out. Fig. 9 illustrates the swelling ratio of the samples as (%*W*) and (%*V*) along incubation time. The swelling ratio (%*W*) curves show a fast increase of water absorption in the first 15 min. A slight increment of water content is observed during the following 24 h of assay. DA-(HA/β-TCP)/Aga-FD samples absorb the greater content of water, followed by DA-(HA/β-TCP)/Aga-RT and (HA/β-TCP)/Aga-RT. The swelling ratio (%*V*) curves show a high volume increase

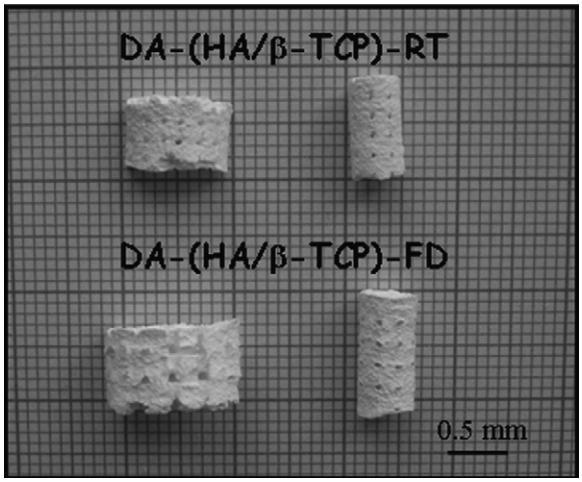

Fig. 8. DA-(HA/β-TCP)/Aga-RT and DA-(HA/β-TCP)/Aga-FD porous scaffolds of different dimensions, after epoxy resin elimination and drying.

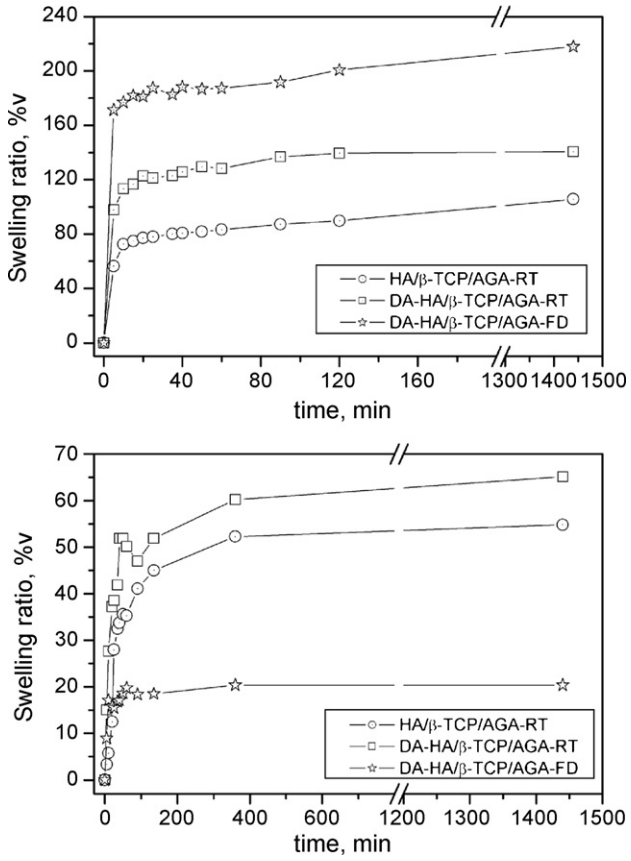

Fig. 9. Swelling ratio (%*W* and %*V*) of scaffolds as a function of incubation time.

during the first 60 min for DA-(HA/β-TCP)/Aga-RT and (HA/β-TCP)/Aga-RT samples. However, DA-(HA/β-TCP)/Aga-FD is observed to gain the maximum volume in the first 15 min. Once the swelling ratio equilibrium is reached, DA-(HA/β-TCP)/Aga-RT is found to be the sample with the higher gained volume followed by (HA/β-TCP)/Aga-RT and (HA/β-TCP)/Aga-FD. These differences between swelling ratios (%*W*) and (%*V*) are explained by the different shrinkage behaviour of the scaffolds.

Fig. 10 illustrates the calculated shrinkage as (%*W*) and (%*V*) of the samples. All the samples experience a similar weight loss. However, the volume loss for DA-(HA/β-TCP)/Aga-FD is a 47% approximately lower compared to (HA/β-TCP)/Aga-RT and DA-(HA/β-TCP)/Aga-RT. This can be explained on the basis of SEM micrographs and mercury intrusion porosimetry. The pore size distribution of DA-(HA/β-TCP)/Aga-FD shows an extra pore size in the range 10–100 μm and a higher total porosity when compared with the rest of the samples as can be seen in Figs. 6 and 7.

The effect of the different drying technique and the designed architecture on water absorption capacity of the ceramic/agarose scaffolds is shown in Fig. 10. On the one hand, the rehydration capacity of scaffolds in terms of (%*W*) is maximal when the freeze-drying technique is employed. On the other hand, the maximum volume regained considerably decreases for FD with regard to RT scaffolds. This is due to the quite similar dimensions of FD scaffolds compared with the just prepared scaffolds. The differences in swelling retaining capability and pore size enlargement displayed by scaffolds dried at RT and FD may be ascribed to different degree of porosity, pore size distribution and interconnectivity [37,38]. This is confirmed by Hg porosimetry and SEM. In addition, the lower volume regained can be explained in terms of quite similar dimensions of DA-(HA/β-TCP)/Aga-FD and just prepared scaffolds.

Scaffolds with designed and non designed architecture dried at RT exhibit similar shrinkage behaviour. However, the water absorption capacity of DA-(HA/β-TCP)/Aga-RT is 23 wt.% and 16 vol.% higher than that of (HA/β-TCP)/Aga-RT. This can be again attributed to the higher porosity and pore size of designed architecture scaffolds.

All these results confirm that the combination of low temperature shaping and stereolithography methods is an excellent

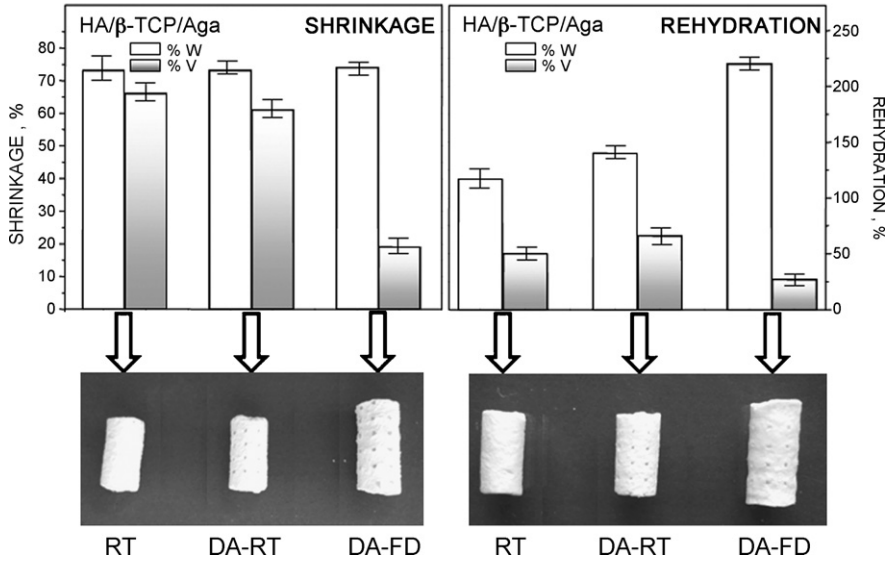

Fig. 10. Shrinkage and rehydration assays of (HA/β-TCP)/Aga-RT (RT), DA-(HA/β-TCP)/Aga-RT (DA-RT) and DA-(HA/β-TCP)/Aga-FD (DA-FD) in weight (%*W*) and volume (%*V*) after 24 h.

alternative for obtaining three-dimensional designed porous architecture scaffolds for tissue engineering applications with at least one ceramic component. Indeed, the exclusive use of low temperature shaping method leads to non designed architecture scaffolds, very useful for many clinical applications, although inappropriate as scaffolds for tissue engineering. Nevertheless, the previous development of a low temperature shaping method that avoids sintering and crystal growth of the ceramic component is essential in order to achieve an effective combination of both methods. At this stage, the knowledge of the optimal experimental conditions for the manufacturing of these non designed architecture scaffolds allows us to easily expand this system towards the manufacturing of high porosity and interconnected pore network scaffolds as it is described in the present work. For this purpose, finding a polymeric substrate acting as negative in the manufacturing of these porous scaffolds is the only requirement. This polymeric negative must be easily removed by chemical methods which must not affect the chemical composition of the ceramic/agarose mixture used. Therefore, this innovative method for the manufacturing of pieces at low temperature allows obtaining scaffolds with a maximal total porosity of 80% and pore sizes distributed in sizes of less than 1 μm, between 1 and 20 μm and between 100 and 460 μm, hence appropriate for bone tissue engineering.

In order to evaluate the biocompatibility of this agarose/ceramic system, mouse L929 fibroblast and human Saos-2 osteoblast have been tested on the scaffolds during different collonization times. The results demonstrate that both cell types adhere and proliferate on the biomaterial surface maintaining their characteristic morphology. [39].

It is worth mentioning that the drying technique employed in the preparation of scaffolds also plays an important role because it affects their porosity. Indeed, DA-(HA/β-TCP)/Aga-RT scaffolds show 63% of total porosity compared to DA-(HA/β-TCP)/Aga-FD scaffolds showing a total porosity of up to 80%.

4. Conclusions

In order to optimise the processing conditions, the maximal amount of HA/β-TCP homogeneously dispersed in the binder solution has been adjusted to achieve dense and defect-free pieces.

Designed architecture porous scaffolds have been developed by combining a low temperature shaping method with stereolithography and two drying techniques obtaining strong dried scaffolds with controlled and complete interconnection, high porosity, thoroughly open pores and tailored pore size. Besides, it has been shown that depending on the drying technique employed, different porosity can be achieved.

This shaping method allows manufacturing scaffolds of different shapes and geometries. Besides, their flexibility and their capacity to exert pressure into the defect in contact with body fluids make them to perfectly fit in the bone defect of the patient and be easily handled by the surgeon.

Finally, the designed architecture FD scaffolds allow the retention of almost all the original properties of just prepared scaffolds.

Acknowledgements

Financial support by the Spanish CICYT (Mat2005-01486) and CAM P-Mat-000324-0505 is gratefully acknowledged. Authors also thank C.A.I. electron microscopy and C.A.I. X-ray diffraction (UCM) for valuable technical and professional assistance.

References

[1] J.M. Karp, P.D. Dalton, M.S. Shoichet, Scaffolds for tissue engineering, MRS Bull. (2003) 301–306.
[2] P.S. Eggli, W. Muller, C.R.K. Schenk, Porous hydroxyapatite and tricalcium phosphate cylinders with two different pore size ranges implanted in the cancellous bone of rabbits, Clin. Orthop. 232 (1988) 127–138.
[3] M. Doblaré, J.M. García, M.J. Gómez, Modelling bone tissue fracture and healing: a review, Eng. Fract. Mech. 71 (2004) 1809–1840.
[4] J.J. Klawitter, S.F. Hulbert, Application of porous ceramics for the attachment of load bearing orthopaedic applications, J. Biomed. Mater. Res. Symp. 2 (1971) 161–229.
[5] O. Gauthier, J.M. Bouler, E. Aguado, P. Pilet, G. Daculsi, Macroporous biphasic calcium phosphate ceramics: influence of macropore diameter and macroporosity percentage on bone ingrowth, Biomaterials 19 (1998) 133–139.
[6] J.X. Lu, B. Flautre, K. Anselme, P. Hardouin, Role of interconnections in porous bioceramics on bone recolonization in vitro and in vivo, J. Mater. Sci.: Mater. Med. 10 (1999) 111–120.
[7] M. Vallet-Regí, Revisiting ceramics for medical applications, Dalton Trans. (2006) 5211–5220.
[8] D.M. Liu, Fabrication of hydroxyapatite ceramic with controlled porosity, J. Mater. Sci.: Mater. Med. 8 (1997) 227–232.
[9] D.M. Liu, Fabrication and characterization of porous hydroxiapatite granules, Biomaterials 17 (1996) 419–421.
[10] L.M. Rodríguez, M. Vallet-Regí, J.M.F. Ferreira, Fabrication of porous hydroxyapatite bodies by a new direct consolidation method: starch consolidation, J. Biomed. Mater. Res. 60 (2002) 232–240.
[11] H. Ramay, M. Zhang, Preparation of porous hydroxyapatite scaffolds by combination of the gel-casting and polymer sponge methods, Biomaterials 24 (2003) 3293–3302.
[12] S. Padilla, J. Roman, M. Vallet-Regí, Synthesis of porous hydroxyapatite by combination of gelcasting and foams burn out methods, J. Mater. Sci.: Mater. Med. 13 (2002) 1193–1197.
[13] P. Sepúlveda, Properties of highly porous hydroxyapatite obtained by the gelcasting of foams, J. Am. Ceram. Soc. 83 (2000) 3021–3024.
[14] A.J. Slosarczyk, Porous hydroxyapatite ceramics, Mater. Sci.: Mater. Med. 18 (1999) 1163–1165.
[15] S. Padilla, S. Sánchez-Salcedo, M. Vallet-Regí, Bioactive glass as precursor of designed-architecture scaffolds for tissue engineering, J. Biomed. Mater. Res. 81A (2007) 224–232.
[16] M. Vallet-Regí, J. González-Calbet, Calcium phosphates in the substitution of bone tissue, Prog. Sol. State Chem. 32 (2004) 1–31.
[17] K.F. Leong, Solid freeform fabrication of three-dimensional scaffolds for engineering replacement tissues and organs, Biomaterials 24 (2003) 2363–2378.
[18] M. Bohner, Physical and chemical aspects of calcium phosphates used in spinal surgery, Eur. Spine J. 10 (2001) S114–S121.
[19] J.M. Bouler, O. Gauthier, Macroporous biphasic calcium phosphates ceramics: influence of five synthesis parameters on compressive strength, Biomaterials 19 (1998) 133–139.
[20] R.Z. LeGeros, J.P. LeGeros, Calcium phosphate biomaterials in medical application, Bioceramics 9 (1996) 7–10.
[21] E.W.H. Bodde, J.G.C. Wolke, R.S.Z. Kowalski, J.A. Jansen, Bone regeneration of porous β-tricalcium phosphate (ConduitTM TCP) and of biphasic calcium phosphate ceramic (Biosel®) in trabecular defects in sheep, J. Biomed. Mater. Res. (2007), doi:10.1002/jbm.a.30990J.

[22] A.C. Jen, C. Wake, A.G. Mikos, Hydrogels for cell immobilization, Biothech. Bioeng. 50 (1996) 357–364.
[23] J.L. Drury, D.J. Mooney, Hydrogels for tissue engineering: scaffold design variables and applications, Biomaterials 24 (2003) 4337–4351.
[24] S. Sánchez-Salcedo, I. Izquierdo-Barba, D. Arcos, M. Vallet-Regí, In vitro evaluation of potential calcium phosphate scaffolds for tissue engineering, Tissue Eng. 12 (2006) 279–290.
[25] M. Vallet-Regí, Bone repair and regeneration possibilities, Mat.-wiss. u. Werkstofftech 37 (2006) 478–484.
[26] A.C. Hull, Apparatus for production of three-dimensional objects by stereolithography, US Pat No. 4575330 (1986).
[27] J. Rodríguez-Carvajal, Recent advances in magnetic structure determination by neutron powder diffraction, Physica B 192 (1993) 55–69.
[28] M.I. Kay, R.A. Young, A.S. Posner, Crystal structure of hydroxyapatite, Nature 204 (1964) 1050–1052.
[29] M. Yashima, A. Sakai, T. Kmiyama, A. Hoshikawa, Crystal structure analysis of β-tricalcium phosphate $Ca_3(PO_4)_2$ by neutron powder diffraction, J. Solid State Chem. 175 (2003) 272–277.
[30] S.V. Dorozhkin, Calcium orthophosphates, J. Mater. Sci. 42 (2007) 1061–1095.
[31] L.L. Hench, J. Wilson, An Introduction to Bioceramics, vol. 1, 1996, p. 1635.
[32] B.S. Chang, C.K. Lee, K.S. Hong, H.J. Youn, H.S. Ryu, S.S. Chung, K.W. Park, Osteoconduction at porous hydroxypaptite with various pore configurations, Biomaterials 21 (2000) 1291–1298.
[33] Z. Xiong, Y. Yan, R. Zhang, L. Sun, Fabrication of porous poly(L-lactic acid) scaffolds for bone tissue engineering via precise extrusion, Scripta Mater. 45 (2001) 773–779.
[34] S. Deville, E. Saiz, A.P. Tomsia, Freeze casting of hydroxyapatite scaffolds for bone tissue engineering, Biomaterials 27 (2006) 5480–5489.
[35] Y.L. Kuen, J.M. David, Hydrogels for tissue engineering, Chem. Rev. 101 (2001) 1869–1879.
[36] A. Hoffman, Hydrogels for biomedical applications, Adv. Drug Deliver. Rev. 43 (2002) 3–12.
[37] A. Sannino, P.A. Netti, G. Mensitieri, L. Nicolais, Designing microporous macromolecular hydrogels for biomedical applications: a comparison between two techniques, Compos. Sci. Technol. 63 (2003) 2411–2416.
[38] W. Friess, J. Werner, Biomedical applications, in: F. Schüth, K.S.W. Sing, J. Weitkamp (Eds.), Handbook of Porous Solids, vol. 5, Wiley-VCH, Germany, 2002, p. 2923.
[39] M. Alcaide, M.C. Serrano, R. Pagani, S. Sánchez-Salcedo, A. Nieto, M. Vallet-Regí, M.T. Portolés, J. Biomed. Mater. Res., submitted for publication.